Superconducting Nanowire Photon-Counting Detectors for Optical Communications

PHOTON-COUNTING DETECTORS can be used in optical communications links to provide a large enhancement in receiver sensitivity over conventional photodetectors at near-infrared wavelengths (1.3–1.55 microns) [1]. However, the highest data rate that has been demonstrated to date using these techniques is about 100 kbits/sec for a receiver consisting of a single InGaAs avalanche photodiode (APD), with projected maximum data rates for large arrays of these detectors in the tens of Mbits/sec [2, 3]. These data rates were limited by the intrinsic few hundred picosecond timing resolution and few nanosecond reset time of the APDs themselves. Applications in which higher data rates are required (and where size, weight, and power [SWAP] limitations for the laser transmitter and/or receiver necessitate a trade-off between SWAP and data rate) therefore constitute a new area of application parameter space for photon-counting receivers, which has heretofore remained inaccessible to current photon-counting detector technologies.

Recently, however, a new technology based on superconducting NbN nanowires [4] was demonstrated, which has shown promise for providing access to this regime. These devices have previously demonstrated a timing resolution of less than 50 psec, and detection efficiencies at 1550 nm as high as approximately 5% [4]. In this article, we present an overview of the ongoing effort at MIT to develop this detector technology into a practical solution for high-sensitivity, high-data-rate, photon-counting optical communications. This effort involves the Optical Communications Technology group at Lincoln Laboratory and the Quantum Nanostructures and Nanofabrication group in the MIT Research Laboratory of Electronics, and combines advanced electron-beam nanofabrication techniques with comprehensive high-speed electrical, optical, and communications testing capabilities. In the past year, our effort has progressed on several fronts, as discussed below, including (1) significant improvements to device fabrication and optical design, yielding detection efficiencies of up to 57% at 1550 nm [5]; (2) experimental investigation and quantitative modeling of the device recovery after a photon detection event [6]; and (3) direct demonstration of detector performance in a photon-counting optical communications link at data rates up to about 780 Mbit/sec for a single device [7].

Detector Operation

Each detector consists of a single superconducting nanowire, so named because of its small size—in our case only 4 nm thick and 100 nm in width. The wire is cryogenically cooled to about 2 to 4 K, well below its critical temperature T_C (which for our NbN devices is around 10 K). Below T_C the wire is superconducting and has essentially zero electrical resistance, while above T_C the wire is in its normal (non-superconducting) state, in which it has a relatively high electrical resistance. The wire is biased with a direct current (DC) density near, but slightly below, the so-called critical current density J_C, above which the superconductivity breaks down. When a photon is absorbed by the wire, as illustrated in Figure 1(a), a small, localized region known as a *hot spot* is created, within which the temperature of the electrons is sufficiently elevated that the superconductivity is disrupted and the material reverts to the normal state. This hot spot is then

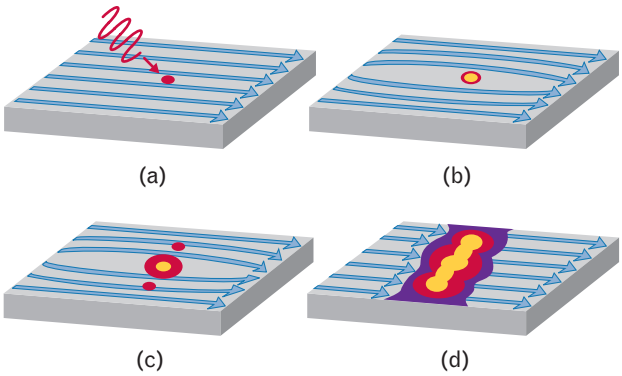

FIGURE 1. Mode of operation of the superconducting nanowire photon counter. (a) A photon is incident upon a nanowire biased with a direct current near the critical current value above which the material is no longer superconducting. (b) A localized hot spot forms where the superconductivity is disrupted by the photon-absorption-induced heating, and the supercurrent diverts around this spot. (c) For a sufficiently narrow wire, the local current density on either side of the hot spot exceeds the critical current density, causing a resistive region to span the entire cross section of the nanowire. (d) A voltage develops across this resistive region, which can be detected electrically.

highly resistive, and the supercurrent diverts around it, as shown in Figure 1(b). Although this region is very small (it has been estimated to be on the order of 10 nm in diameter for a near-infrared photon [8]), its presence can be detected electrically if the wire is sufficiently narrow, and for an initial DC current density J close enough to the critical value J_C. In this case, the occurrence of the hot spot can cause J to exceed J_C locally as the charge carriers moving around the spot are forced both to accelerate and to increase in density, as shown in Figure 1(c). This can result in disruption of superconductivity throughout an entire cross section of the wire, as shown in Figure 1(d), and the consequent appearance of a voltage across the wire, which can be detected electrically [9, 6].

Detection Efficiency

Because NbN is highly resistive at optical frequencies (approximately 150 times higher than copper) it is a very good optical absorber, with a 4-nm-thick film having about 45% absorption at 1550 nm. However, it is a significant technical challenge to take advantage of this high absorption in a nanowire photon counter. First, the wire must be extremely narrow (as mentioned above), much smaller than the wavelengths of

SUPERCONDUCTIVITY

The phenomenon of superconductivity was first observed in 1911 by Gilles Holst and Heike Kammerlingh-Onnes in their laboratory in Leiden, the Netherlands. When a thin capillary tube of mercury was cooled below a temperature of about 4.2 K by immersing it in a bath of liquified helium, its electrical resistance was observed to become immeasurably small. The transition to this state occurred not gradually, as had been expected because of the removal of any remaining thermal fluctuations, but *suddenly* at a very specific and well-defined temperature. We now understand this to be a thermodynamic phase transition, and the temperature at which it occurs is known as the superconducting transition temperature T_C [1].

Superconductivity can be characterized by two physical properties: (1) zero direct current (DC) electrical resistivity; and (2) perfect diamagnetism (shielding of external, static magnetic fields). These are conventionally expressed in a form known as the London equations, after the brothers F. and H. London, who posited them in 1935 as a phenomenological description of experimental observations [2], decades before their microscopic origin was understood in terms of the BCS theory of superconductivity [3]. The London equations are

$$\mathbf{E} = \frac{\partial}{\partial t}(\lambda^2 \mu_0 \mathbf{J}) \qquad (1)$$

$$\nabla \times (\lambda^2 \mu_0 \mathbf{J}) = -\mathbf{B} \qquad (2)$$

Here, **E** and **B** are the electric and magnetic fields, respectively, **J** is the current density, μ_0 is the per-

meability of free space, and λ is known as the magnetic penetration depth.

Equation 1 shows that a fixed electric field will cause an accelerating increase in the current, which implies zero resistivity. Furthermore, it also contains the effect of the kinetic inductance (which is important for our nanowires), which essentially arises from the inertia of the accelerated current density (or equivalently, from the kinetic energy stored within it). Equation 2 shows that static magnetic fields are excluded from the bulk of a superconductor, except within a distance λ from the surface, where superconducting screening currents flow. These currents produce a magnetic field exactly canceling the external field in the interior of the sample. This effect is outwardly similar to the well-known skin effect in ordinary metals, in which alternating currents and fields penetrate only near the surface (for a superconductor this effect occurs even at DC). A consequence of this effect, which is important for structures like our nanowires having dimensions much smaller than λ (effectively a few tens of microns for our thin NbN films) is that the magnetic field and current density are uniform throughout the material. The current does not flow only on the surface as it would in a bulk superconductor.

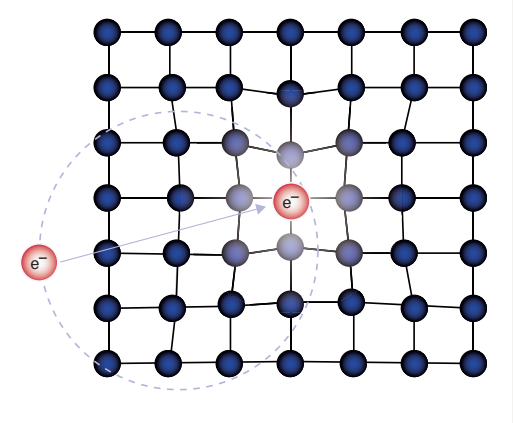

FIGURE A. The attractive interaction between electrons in a solid results in Cooper pairing and superconductivity. One electron electrostatically distorts the charge distribution of the nearby ions; this distortion can be thought of as excitation of lattice vibrational modes, or *phonons*. A nearby electron is attracted to this distortion of the lattice because of the localized increase in positive charge density, which can be described as arising from phonon exchange.

The properties described by Equations 1 and 2 have their origins in the fundamentally quantum-mechanical nature of the superconducting state itself, which is conceptually distinct from what we would obtain by considering a metallic conductor and taking the limit where its resistance goes to zero. At the heart of this quantum-mechanical state is a phenomenon known as *Cooper pairing* [2, 3], illustrated in Figure A. A given pair of electrons in a solid, whose mutual interaction is normally repulsive (though it is reduced due to screening by all the other nearby electrons) can under the right circumstances have an effectively attractive interaction, when we include the effect of the coupling of the pair to vibrations of the underlying lattice of ions. A given electron temporarily distorts the ionic lattice as it moves, in a similar way to a heavy ball moving on a flexible membrane. That distortion can then itself produce a transient force on a second electron that is nearby, which pulls it toward the first electron. In this manner, an attractive force between electrons is said to be present, and mediated by phonons (the quanta of lattice vibration) exchanged between the interacting electrons. This is analogous to, for example, the manner in which attractive van der Waals forces between atoms are said to be mediated by exchanged photons. Just as in that case, where molecules can form due to the attractive interatomic interactions, so in the case of a superconductor can bound pairs of electrons be formed; these are known as Cooper pairs.

However, a very important difference exists in the latter case. As shown in parts *a* and *b* of Figure B, the electronic structure of semiconductors and metals is fundamentally related to the quantum statistics of the electrons. Because they are spin-½ fermions that must obey the Pauli exclusion principle, no more than one electron can occupy each available quantum state. This results in a filling of the available states by the total number of electrons in the system, up to an energy known as the Fermi level. When electrons bind together into Coo-

per pairs, however, they begin to act like bosons (with total spin zero, for most superconductors). Since each bound pair's energy is lower than that of two individual electrons (by the binding energy) and since as bosons the pairs are no longer restricted from occupying the same quantum state, they tend to condense together into this lower energy state, a phenomenon known as Bose-Einstein condensation. In this way a gap opens in the single-particle excitation spectrum, near the Fermi energy, as shown schematically in part *c* of Figure B. In the superconducting state, the lowest-lying single-particle excitations then involve breaking at least one Cooper pair, and therefore require at least the pair binding energy to be excited. This energy is of the order of $k_B T_C$, or about 1 meV for typical elemental metallic and simple alloy superconductors.

In a qualitative sense, this explains why a superconductor can make a sensitive photodetector, as illustrated in Figure B. In a conventional semiconductor material (as in, for example, a silicon photodiode) the relevant energy gap is between the valence and conduction bands of the material, which is on the order of 1 eV. An incident optical photon (also about 1 eV energy) excites an electron across this gap, and the resulting electron-hole pair is measured electrically as a current. In the superconductor, an optical photon initially excites only one electron (breaks one Cooper pair), and this one electron quickly interacts with and breaks many other Cooper pairs, with the net result that hundreds of excited electrons can build up at the gap edge. In our nanowire detectors, it is precisely these excited electrons that produce the hot spot. The superconducting detector most analogous to the semiconductor photodiode described above is known as a superconducting tunnel junction detector, and it operates by directly reading out these excited electrons as a current.

An interesting consequence of this detection method is that the energy of the incident photon can be measured (or the number of incident photons of a given energy), albeit at relatively slow speeds compared to present nanowire detectors.

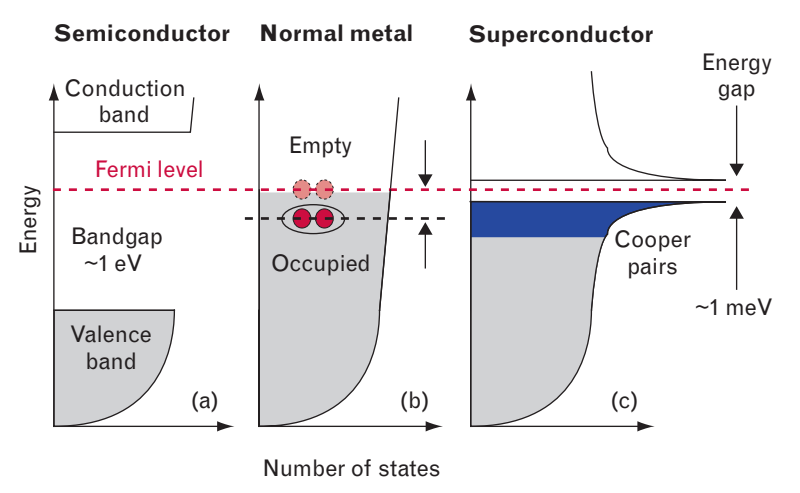

FIGURE B. Simplified single-particle band structure for (a) a semiconductor, (b) a normal metal or a superconductor well above its critical temperature, and (c) a superconductor below its critical temperature. In a semiconductor, electrons fill up just to the top of the valence band, and the lowest-lying electronic excitation is associated with transferring an electron from the valence band to the conduction band. This energy gap is typically around 1 eV and is associated with an atomic-level spacing of the constituent ions that make up the solid. In a normal metal, a conduction band is only partially filled. If the metal is cooled below its superconducting transition temperature, electrons begin to bind together to form Cooper pairs, and the material condenses into the superconducting state. When this occurs, a gap opens in the single-particle excitation spectrum, which is associated with breaking a Cooper pair. This gap is about 1 meV, in contrast to the 1 eV gap of a semiconductor.

References

1. See, for example, M. Tinkham, *Introduction to Superconductivity*, 2nd ed. (Dover, Mineola, N.Y., 1996); T.P. Orlando and K.A. Delin, *Foundations of Applied Superconductivity*, (Addison-Wesley, Reading. Mass., 1991).
2. F. and H. London, "The Electromagnetic Equations of the Supraconductor," *Proc. Roy. Soc. Lond. A* **149** (866), 1935, pp. 71–88.
3. J. Bardeen, L.N. Cooper, and J.R. Schrieffer, "Theory of Superconductivity," *Phys. Rev.* **108** (5), 1957, pp. 1175–1204.
4. L.N. Cooper, "Bound Electron Pairs in a Degenerate Fermi Gas," *Phys. Rev.* **104** (4), 1956, pp. 1189–1190.

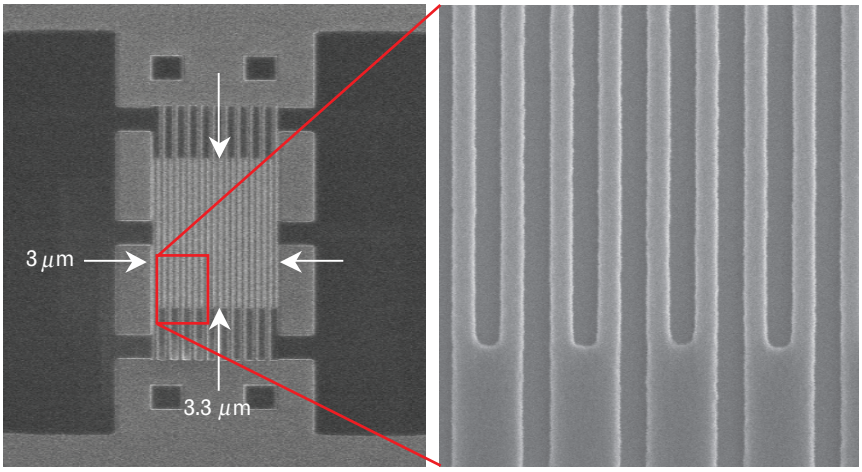

FIGURE 2. Scanning-electron micrograph of the electron-beam resist pattern used to define the meander structure of our detectors. The structure improves the coupling of incident photons onto the nanowire, which is much less than a wavelength in width. This particular device has a wire width of 100 nm, with 100 nm gaps between the wires. Such small (subwavelength) gaps in the absorbing film allow only evanescent-wave penetration of light, and the net absorption of the structure remains high, approximately 35%, compared to approximately 45% for a uniform film.

interest. To achieve efficient coupling of incoming photons onto the wire, the wire is fabricated in a so-called meander pattern [4], as illustrated in Figure 2 for a detector with an active area of 3 μm × 3.3 μm, consisting of a single 100-nm-wide wire with 100 nm gaps between sections (50% fill factor). Because of the subwavelength size of the gaps, the net reduction in absorption of this structure relative to a uniform film is significantly smaller than the factor of two that would result from large gaps but with the same fill factor. Calculations indicate that the intrinsic 45% absorption should be reduced only to about 35% for this configuration. (Note that we include the whole area of the meander structure, including the gaps, in our definition of active area.) Although this type of pattern is well known in other types of superconducting electronics, it is a significant technical challenge to make such a pattern on these nanometer-length scales, with acceptable device yields. The present successful devices are the result of a major effort in nanofabrication process development by the MIT Quantum Nanostructures and Nanofabrication group [10, 5].

A second important method for improving the detection efficiency involves taking maximum advantage of the 35% absorption of the meander structure. This method has to do with the quality of the meander pattern itself, specifically, the uniformity of the wire width along its length. If, for example, a small section of the wire is narrower than the rest, it will limit the current that can be sent through the wire, since the current density will always be highest at this weak link. To have high detection efficiency, however, the current bias must be as close as possible to the critical value. Therefore, any localized narrowing of the wire will translate directly into a lower detection efficiency, resulting in the low initial values on the order of 5% at 1550 nm. For this reason, the electron-beam patterning process developed by the MIT Quantum Nanostructures and Nanofabrication group has been designed specifically to minimize line-edge roughness [10]. This improved capability has resulted in detection efficiencies at 1550 nm as high as 21% for 4-nm-thick films. In addition, it has greatly improved the yield of high-efficiency devices; for 130 identical devices on a single chip, the median detection efficiency was 17%.

The final contribution to maximizing the detection efficiency involves going beyond the limitation imposed by the approximately 35% single-pass absorption of our 4 nm meander structures by using a microfabricated optical cavity, as shown in Figure 3. A glass spacer is patterned directly on top of the detector, followed by a gold mirror. The device is then illuminated from the back, through the sapphire substrate. By correctly choosing the thickness of the spacer, we can arrange for destructive optical interference between the primary reflection from the NbN/sapphire interface and the reflection from the back mirror. In this way, the net reflection and transmission of the entire structure are minimized, increasing the absorption in the NbN film. By using this technique, we have achieved detection efficiencies as high as 57% at 1550 nm, with a median over 130 devices of 47% [5]. On the basis of this data, we can say with confidence that the prospects for making small arrays of these high-efficiency devices are already quite good.

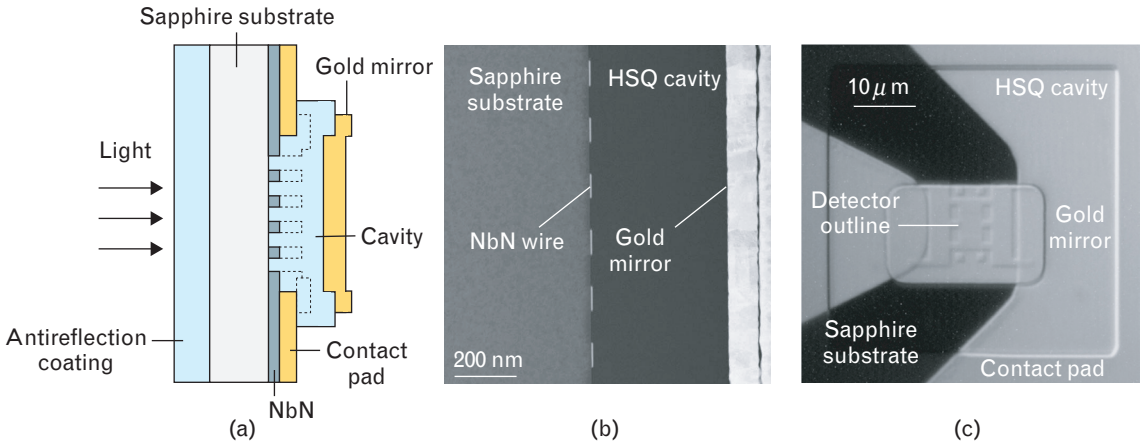

FIGURE 3. Enhancement of NbN film absorption due to microfabricated optical coupling structure. (a) Schematic of the structure: a glass spacer is deposited on top of the NbN detector followed by a gold mirror. The thickness of the spacer is chosen (about 200 nm) such that destructive interference occurs between light reflected from the NbN/sapphire interface and that reflected from the mirror, maximizing the net absorption in the thin film. In addition, an anti-reflection coating is deposited on the back of the sapphire substrate to reduce the Fresnel reflection loss of approximately 7.5% that would otherwise result at the vacuum/sapphire interface. (b) Transmission electron micrograph of the cross section of the structure. (c) Top-view optical micrograph of the integrated device, showing the outer electrical contact pads, and the outlines of the glass spacer and gold mirror.

Reset Time

The reset time of a photon counter is the delay after a detection event before the next photon can be detected. Although the timing resolution sets the fundamental bandwidth limitation of a photon-counting receiver, the reset time is also important, since it determines how large an array will be required to take full advantage of the intrinsic timing resolution. A long reset time means that many detectors will have to be used in parallel to avoid so-called blocking loss associated with the fraction of the time that each detector is recovering from a previous detection event and remains insensitive to incoming photons. Although very high timing resolution (less than 50 psec) had been demonstrated for this technology some years ago [4], virtually nothing was known about their reset time prior to this work.

To measure the reset time, we illuminated test devices with optical pulse pairs, with the first pulse inducing a detection event, and the second pulse probing the instantaneous detection efficiency at an adjustable later time. Figure 4 uses solid and open circles to show the results for two different detectors; solid lines show the predictions of our electrical model of the device recovery for the same two detectors, with no free parameters [6]. At the heart of this model is the idea that the recovery time of these devices is limited by a time constant associated with their so-called kinetic inductance, which for a typical 3 μm × 3.3 μm device results in a reset time of about 3.5 nsec (defined by the time required for the detection efficiency to return to 90% of its initial value). Kinetic inductance is associated with the fact that in a superconductor the charge carriers move freely, without resistance, and can therefore store (kinetic) energy reversibly in an analogous way to the storage of energy in the magnetic field of an inductor; electrically, the two are indistinguishable [11]. For very thin films such as ours, however, the kinetic inductance can be orders of magnitude greater than the magnetic inductance of the same structure. For example, the kinetic inductance of one of our 3 μm × 3.3 μm devices is about 50 nH, while the magnetic inductance is estimated to be less than 1 nH. Because kinetic inductance is proportional to the total wire length, an important trade-off occurs for these devices (at least in the present configuration) between active area and reset time. This fact is illustrated by the two sets of data, and corresponding theoretical curves in Figure 4, which are for two devices having total wire lengths of 120 μm and 60 μm, and corresponding kinetic inductances of 109 nH and 47.1 nH. These cor-

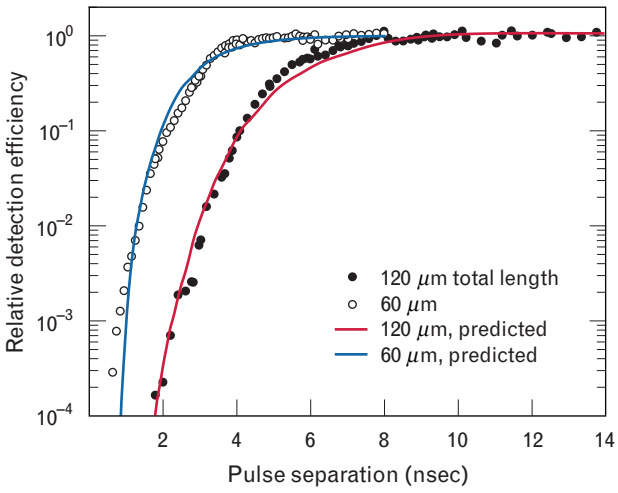

FIGURE 4. Recovery of the nanowire device after a photon detection event. Two devices cooled to 4.2 K were illuminated with optical pulse pairs; the first caused the device to fire, while the second probed the instantaneous detection efficiency as a function of time after the device fired. Solid circles are results for a device having total wire length of 120 μm (corresponding to an active area of 4 μm × 6 μm) while open circles are for a 60-μm-long wire. The recovery time of the detection efficiency is governed by the intrinsic kinetic inductance of the nanowires, which is proportional to their total length. The solid curves are predictions, with no free parameters, based on independently measured device parameters, and an electrical model of the device operation including kinetic inductance.

respond to effective active areas of 4 μm × 6 μm and 3 μm × 4 μm, respectively.

Photon-Counting Communications Demonstration

The combination of a timing resolution less than 50 psec and a recovery time of a few nanoseconds allows these NbN nanowire detectors to operate in a regime of data transmission rates previously unattainable in photon-counting optical communications. To demonstrate this, we have integrated one of these devices into our existing photon-counting optical communications testbed, which incorporates a pulse-position modulation (PPM) signaling format with advanced forward-error-correction codes developed for deep-space photon-counting communications applications, and capable of operating very close to theoretical optimum channel capacity [12]. Based on the 50 psec timing jitter inherent in the detector and readout electronics, a minimum PPM slot width of 100 psec was used (to avoid large penalties due to inter-symbol interference). The PPM order was 32 (slots per symbol), so that each detected pulse then conveyed $\log_2 32 = 5$ bits of information, 2.5 of which were source data, and 2.5 of which were overhead used for error correction. This yields a source data rate of 2.5 bits/3.2 nsec = 781.25 Megabits/sec, nearly a factor of 10,000 improvement over previously demonstrated photon-counting communications data rates [3]. Figure 5 shows the bit error rate (BER) as a function of detected photons per

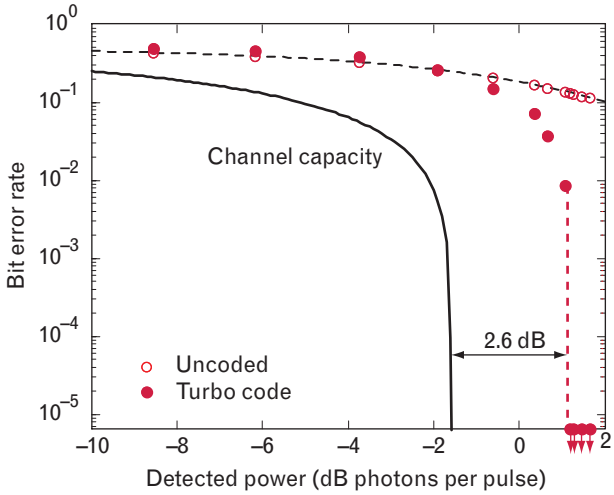

FIGURE 5. Demonstrated photon-counting communications performance of a NbN nanowire detector at 1.8 K. This experiment was carried out by using 32-ary pulse-position modulation with a 100 psec slot period (3.2 nsec symbol length). An early device used in the experiment did not incorporate the integrated cavity structure, and had a detection efficiency at 1.8 K of about 7%. Open circles show the bit error rate as a function of detected power in photons per pulse, and the dotted line is a fit to the expected error rate, based on Poisson photon-counting statistics. The filled circles show the bit error rate with forward error correction, which exhibits the characteristic sudden dropoff at a threshold value of detected photons at which the error rate goes to unmeasurably small values (where the measurement is limited only by the amount of data transmitted). The number of detected photons at which this threshold occurs is therefore the minimum necessary to close the link. It occurs at about 1.2 photons per pulse, corresponding to about 2.0 bits per detected photon. The solid line is the limitation imposed by the theoretical channel capacity. The discrepancy of 2.6 dB between the measured value and capacity is larger (by about 1 dB) than has been previously demonstrated with these techniques. This difference is most likely due to the increased effects of detector jitter and blocking (due to the device's 3 nsec reset time) at the very high count rates used in the experiments.

optical pulse (open and filled circles), as well as the theoretical maximum channel capacity (solid line). The coded BER drops quickly to zero above a critical number of detected photons per pulse (a characteristic of the performance of these error-correction codes), corresponding to the minimum number of photons per pulse necessary to close the communications link and obtain error-free performance. In the present case, this minimum number corresponds to a sensitivity of about 2 bits per detected photon. The performance is limited in part by several effects, including blocking loss due to the reset time of the detector and errors due to the 50 psec timing jitter, which is significant compared to the 100 psec slot. Work is under way on mitigating these limiting effects, and Gbit/sec data rates are expected in the coming year.

Conclusion

We have shown that superconducting NbN nanowire single-photon counters show great promise in providing access to an entirely new regime in high-sensitivity, Gbit/sec-class photon-counting optical communications. Further improvements in reset time and timing jitter are anticipated, as well as arrays of devices for even higher data rates and spatial acquisition and tracking. Prospects for using these devices in a contemplated 1 Gbit/sec downlink from a lunar transmitter are currently under study. Furthermore, the long-term prospects for using higher-temperature superconducting materials for these devices, as well as for developing superconducting integrated-readout architectures, could allow the applicability and flexibility of these devices to be extended even further.

Contributed by Andrew J. Kerman, Eric. A. Dauler, Bryan S. Robinson, Richard Barron, David O. Caplan, Mark L. Stevens, John J. Carney, Scott A. Hamilton, and William E. Keicher of the Optical Communications Technology group, Lincoln Laboratory, and Joel K.W. Yang, Kristine Rosfjord, Vikas Anant, and Karl K. Berggren of the Quantum Nanostructures and Nanofabrication group, Research Laboratory of Electronics, Massachusetts Institute of Technology, Cambridge, Massachusetts.

REFERENCES

1. J.R. Pierce, "Optical Channels: Practical Limits with Photon Counting," *IEEE Trans. Comm.* **26** (12), 1978, pp. 1819–1821.
2. K.J. Gordon, V. Fernandez, P.D. Townsend, and G.S. Buller, "A Short Wavelength GigaHertz Clocked Fiber-Optic Quantum Key Distribution System," *IEEE J. Quant. Electron.* **40** (7), 2004, pp. 900–908.
3. B.S. Robinson, D.O. Caplan, M.L. Stevens, R.J. Barron, E.A. Dauler, and S.A. Hamilton, "1.5-Photons/Bit Photo-Counting Optical Communications Using Geiger-Mode Avalanche," *2005 Dig. LEOS Summer Topical Mtg, San Diego, 25–27 July 2005,* paper TuA3.1, pp. 41–42**;** B.S. Robinson, D.O. Caplan, M.L. Stevens, R.J. Barron, E.A. Dauler, S.A. Hamilton, K.A. McIntosh, J.P. Donnelly, E.K. Duerr, and S. Verghese, "High-Sensitivity Photon-Counting Communications Using Geiger-Mode Avalanche Photodiodes," *LEOS 2005, 18th Ann. Mtg. of the IEEE Lasers and Electro-Optics Society, Sydney, 23–27 Oct. 2005,* pp. 559–560.
4. R. Sobolewski, A. Verevkin, G.N. Gol'tsman, A. Lipatov, and K. Wilsher, "Ultrafast Superconducting Single-Photon Optical Detectors and Their Applications," *IEEE Trans. Appl. Supercond.* **13** (2), 2003, pp. 1151–1157, and references therein.
5. K.M. Rosfjord, J.K.W. Yang, E.A. Dauler, A.J. Kerman, V. Anant, B.M. Voronov, G.N. Gol'tsman, and K.K. Berggren, "Nanowire Single-Photon Detector with an Integrated Cavity and Anti-Reflection Coating," *Opt. Express* **14** (2), 2006, pp. 527–534.
6. A.J. Kerman, E.A. Dauler, W.E. Keicher, J.K.W. Yang, K.K. Berggren, G. Gol'tsman, and B. Voronov, "Kinetic-Inductance-Limited Reset Time of Superconducting Nanowire Photon Counters," *Appl. Phys. Lett.* **88,** 2006, pp. 111–116.
7. B.S. Robinson, A.J. Kerman, E.A. Dauler, R.J. Barron, D.O. Caplan, M.L. Stevens, J.J. Carney, S.A. Hamilton, J.K.W. Yang, and K.K. Berggren, "781-Mbit/s Photon-Counting Optical Communications Using a Superconducting Nanowire Detector," *Opt. Lett.* **31,** 2006, p. 444.
8. A. Engel, A. Semenov, H.-W. Hübers, K. Il'in, and M. Siegel, "Fluctuations and Dark Count Tates in Superconducting NbN Single-Photon Detectors," *Phys. Stat. Solidi C* **2** (5), 2005, pp. 1668–1673.
9. A.D. Semenov, G.N. Gol'tsman, and A.A. Korneev, "Quantum Detection by Current Carrying Superconducting Film," *Physica C* **351** (4), 2001, pp. 349–356.
10. J.K.W. Yang, E. Dauler, A. Ferri, A. Pearlman, A. Verevkin, G. Goltsman, B. Voronov, R. Sobolewski, W.E. Keicher, and K.K. Berggren, "Fabrication Development for Nanowire GHz-Counting-Rate Single-Photon Detectors," *IEEE Trans. Appl. Supercond.* **15** (2, pt 1), 2005, pp. 626–630.
11. See, for example, T.P. Orlando and K.A. Delin, *Foundations of Applied Superconductivity* (Addison-Wesley, Reading, Mass., 1991).
12. B.E. Moision and J. Hamkins, "Reduced Complexity Decoding of Coded Pulse-Position Modulation Using Partial Statistics," *The Interplanetary Network Progress Report* **42-161,** May 15, 2005.